Efficiency Analysis of An Integrated Cascade Sorption Energy Storage into A Solar DHW System

Nasrin Aliyari[1], Marco S. Fernandes[1], Adélio R. Gaspar[1]

[1] Univ Coimbra, ADAI, Department of Mechanical Engineering, Rua Luís Reis Santos, Pólo II, 3030-788 Coimbra, Portugal

Abstract

Sorption heat storage has garnered significant interest for its potential in long-term thermal energy storage, particularly in domestic hot water (DHW) systems. This paper explores the concepts and operating principles of single material and cascade thermochemical energy storage systems, focusing on their application in solar DHW production. Single material sorption systems store and release energy based on reversible physicochemical phenomena, while cascade systems utilize two different storage materials to optimize energy density and discharge temperature. The study assesses and compares the integration of salt-hydrates-based cascade sorption energy storage, specifically using $MgCl_2 \cdot 6H_2O$ and $SrBr_2 \cdot 6H_2O$, with a solar DHW system for a single-family dwelling in the distinct climates of Coimbra (Portugal) and Shiraz (Iran). The findings indicate that the cascade system can result in a 21% and 43% reduction in auxiliary energy demand respectively in Coimbra and Shiraz, thus significantly increasing the renewable energy share and enhancing energy efficiency in DHW systems.

Keywords: DHW, Thermal storage, Adsorption, Cascade System, Solar energy

1. Introduction

Sorption heat storage has generated much interest due to its potential for long-term thermal energy storage (Scapino *et al.*, 2017). It is a promising technology for enhancing the efficiency and sustainability of energy systems, particularly in the context of building applications. This method leverages the reversible chemical reactions between a sorbent material and water vapor to store and release thermal energy (Fernandes *et al.*, 2016). Salt hydrates, particularly, are highly effective sorbents due to their substantial energy storage densities and favorable thermodynamic properties (Yan and Zhang, 2022). For salt hydrate-based sorption heat storage, salt hydrates form new crystal structures by either dissociating or absorbing water molecules, thereby enabling the storage or release of thermal energy in the form of chemical bonds. The typical reaction can be represented as follows (Stitou *et al.*, 1997; Xu *et al.*, 2021):

$$MX \cdot xH_2O_{(s)} + yH_2O_{(g)} \leftrightarrow MX(x+y) \cdot H_2O_{(s)} + y\Delta H_r \qquad \text{(eq. 1)}$$

Where $MX \cdot xH_2O$ is a salt hydrate produced from the chemical salt MX and solvent H_2O. MX and H_2O constitute the working pair. ΔHr is the enthalpy of the chemical reaction. The operating principle of salt hydrate-based sorption heat storage can be classified into two charging (dehydration) and discharging (hydration) processes. When exposed to heat, salt hydrates undergo a dehydration process, with the desorption heat being stored in the sorbent using a chemical bond. During cooler periods, the stored energy is released as the salts rehydrate, providing a reliable and efficient source of heat. This technology is particularly advantageous for long-term thermal energy storage, as it can be charged during periods of excess energy (such as summer) and discharged during times of high energy demand (such as winter), thereby reducing reliance on auxiliary heating systems and improving overall energy efficiency.

The sorption storage system needs to provide the user with useful discharging temperature and energy storage density. To conciliate the requirement for high energy density and thermodynamic constraints like discharging and charging temperatures, it is possible to utilize two different thermochemical (storage) materials (TCM) in a cascade configuration (N'Tsoukpoe *et al.*, 2016) – one with higher energy storage density but unable to provide the useful discharging temperature (TCM1) and other that can provide the useful temperature level under the set discharging constraints but with lower storage density (TCM2). In the end, the system can satisfy the user with the desired discharging temperature while the overall energy storage density is between the

Selection and/or peer review under responsibility of Scientific Committee
10.18086/eurosun.2024.06.01 Available at http://proceedings.ises.org

respective energy storage densities of the two materials.

The objective of this study is to assess the integration of single material sorption heat storage (Fig. 1a) with a solar DHW production system and compare its performance with a cascade configuration (Fig. 1b), by evaluating the system efficiency in reducing the auxiliary energy demand in relation to the conventional DHW system. The storage unit performs both charging and discharging processes at the same time and at every moment. This assessment is performed for the mild climate of Coimbra (Portugal) and the harsher climate of Shiraz (Iran).

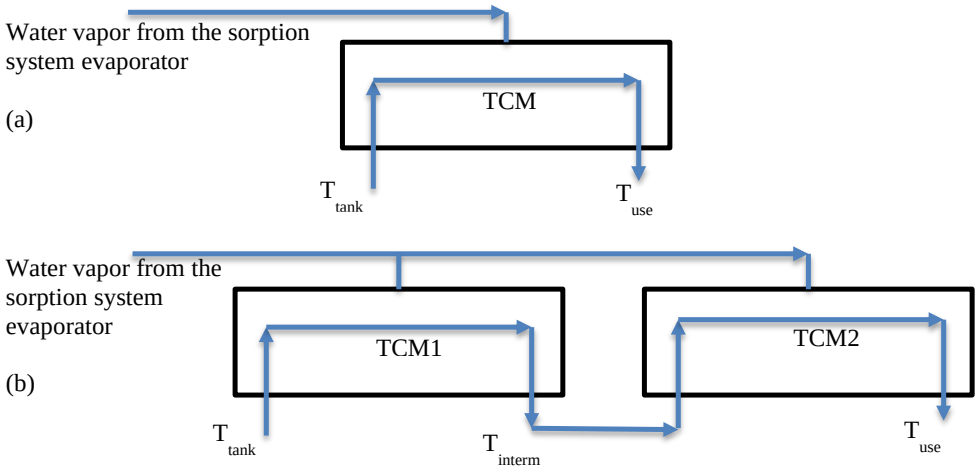

Fig. 1: (a) Single material heat storage configuration; (b) cascade heat storage configuration. T_{tank}, T_{use} and T_{interm} are the minimum outlet temperature of the tank, end-use temperature, and intermediate temperature.

2. Problem Description and Methodology

The auxiliary energy reduction percentage of the solar DHW sorption storage system in relation to the conventional system (without sorption storage) is calculated for two scenarios: (i) integration of a single-material sorption thermal storage, and (ii) integration of a cascade sorption thermal storage. The conventional solar DHW system (**Error! Reference source not found.**) is simulated in TRNSYS 18 to calculate the auxiliary heat (Q_{aux}) required during a year. The simulation is then performed for the integrated solar DHW system (**Error! Reference source not found.**) with single-material and cascade sorption thermal storage under the following thermodynamic constraints:

- For discharge, a minimum temperature of 55 °C has been defined to satisfy the need for DHW.
- The maximum output of the hot water tank has been set to 100 °C, which is adopted as the maximum charging temperature.
- The heat sink provides a condensation temperature of 22 °C and the low-temperature heat source an evaporation temperature of 10 °C.

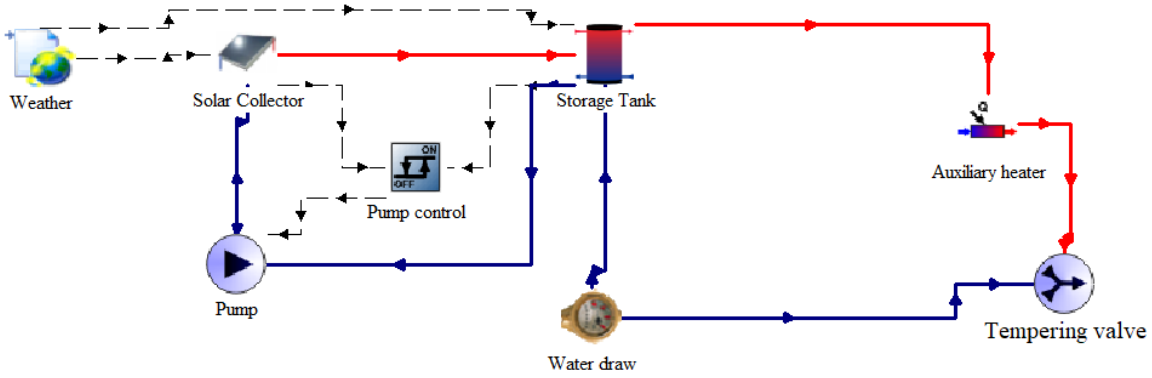

Fig. 2: Conventional solar DHW system.

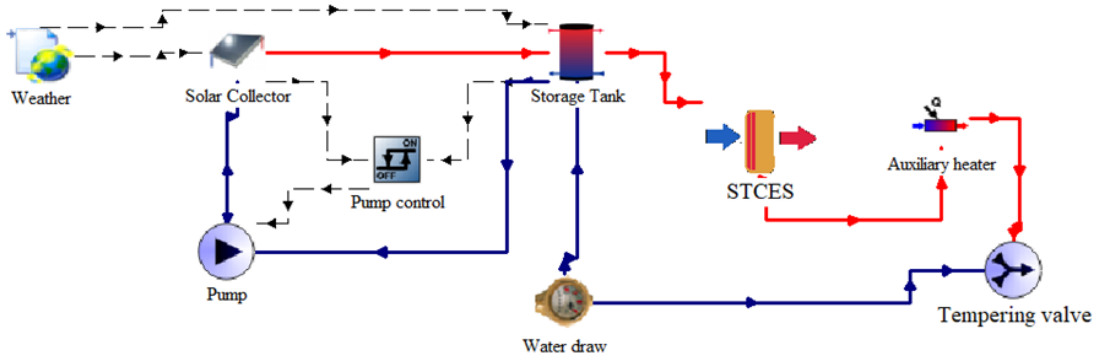

Fig. 3: Solar DHW system integrated with sorption storage unit.

In the conventional system, the outlet flow from the hot water tank, heated by solar energy, flows through the auxiliary heater, where, if the temperature is below the set point at the storage tank outlet, it is heated to reach the desired temperature. In the integrated DHW system with an energy storage unit, the outlet fluid flow from the storage tank first passes through the sorption storage unit (STCES), before entering the auxiliary heater. The thermal energy dynamics of the storage unit, consisting of two TCM, are simulated to manage simultaneous heat storage and release based on the inlet fluid temperature. When the fluid's temperature exceeds 55 °C, the system charges by storing heat in the TCMs, with the amount of stored heat being limited to predefined maximum values of each TCM. Conversely, when the temperature is lower than 55 °C, the system discharges by releasing stored heat to the fluid. The system continuously tracks the total stored, released, and remaining energy, ensuring accurate energy management within the storage unit. This method allows an understanding of the efficiency and behavior of the thermal energy storage system under varying operational conditions.

As for typical domestic hot water consumption patterns, Fuentes *et al.* (2018) provided information for different European countries, referring to a value of 0.04 $m^3\ day^{-1}\ person^{-1}$ for Portugal. **Error! Reference source not found.** illustrates a daily consumption pattern for a single-family of 4 people (0.16 $m^3\ day^{-1}$) considered for both Shiraz and Coimbra, for which the main consumption peaks occur in the morning and the

evening.

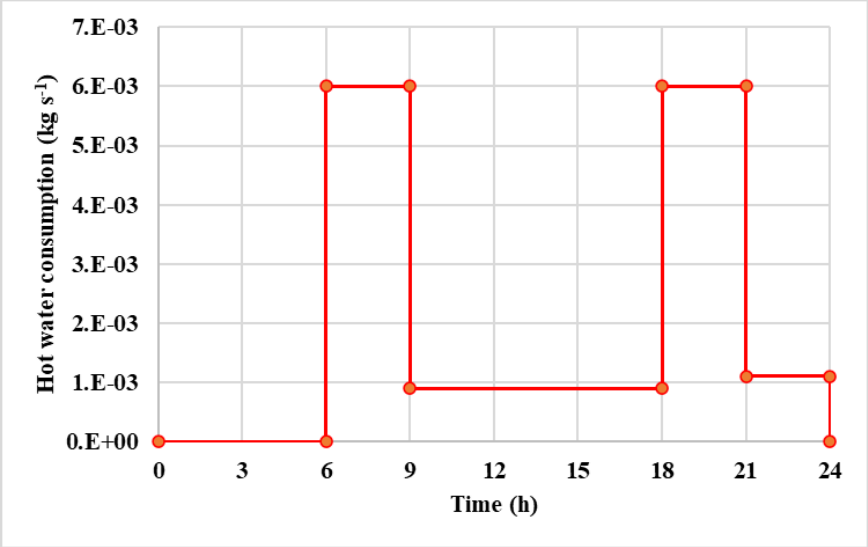

Fig. 4: Daily hot water consumption profile considered for a single-family of 4 people in Coimbra and Shiraz.

The primary task in designing a sorption thermal storage system is to select the appropriate material. Based on the previously mentioned thermodynamic constraints, the selection criteria for the main material are as follows:

- Under a condensation vapor pressure of 2600Pa (26 mbar) (corresponding to the water vapor pressure at 22 °C), the equilibrium temperature of the material should not exceed 100°C, to meet the maximum charging temperature requirement.
- Under an evaporator vapor pressure of 1200 Pa (12 mbar) (corresponding to the water vapor pressure at 10 °C), the equilibrium temperature of the salt should be above 55 °C, to fulfill the requirement of a discharging temperature of at least 55 °C.

The thermodynamics constraints are represented on the equilibrium curves diagram of salt hydrates, Fig. 5. To satisfy both charging and discharging constraints (no. 1 and no. 2), the equilibrium curve of the salt must intersect both the charging and discharging constraint areas. As a result, possible salt hydrates that could be used as primary salt are represented in Tab. 1. Although $Na_2S{\cdot}5\text{-}2H_2O$, with its large energy storage density (D_v), could be the best candidate, its main drawback is its toxicity. Among the other candidates, $MgCl_2{\cdot}6\text{-}4H_2O$ stands out due to its higher energy storage density and appropriate discharging temperature. Therefore, magnesium chloride has been selected as the storage material for the single-material storage system, with an energy storage density of 8.5×10^5 kJ, a charging temperature of 73.8 °C, and a discharging temperature of 60.5 °C.

Tab. 1: Possible salt hydrates to be used as primary salt.

Hydrated Salt	$MgCl_2{\cdot}6H_2O$	$SrCl_2{\cdot}2H_2O$	$Na_2S{\cdot}5H_2O$
Dehydrated Salt	$MgCl_2{\cdot}4H_2O$	$SrCl_2{\cdot}H_2O$	$Na_2S{\cdot}2H_2O$
$T_{melting}$ [°C]	117	100	70.8
T_{disch} [°C]	60.5	58	65.8
T_{charge} [°C]	73.8	70	77.9
D_v [kJ m^{-3}]	8.5×10^5	8.1×10^5	1.8×10^6

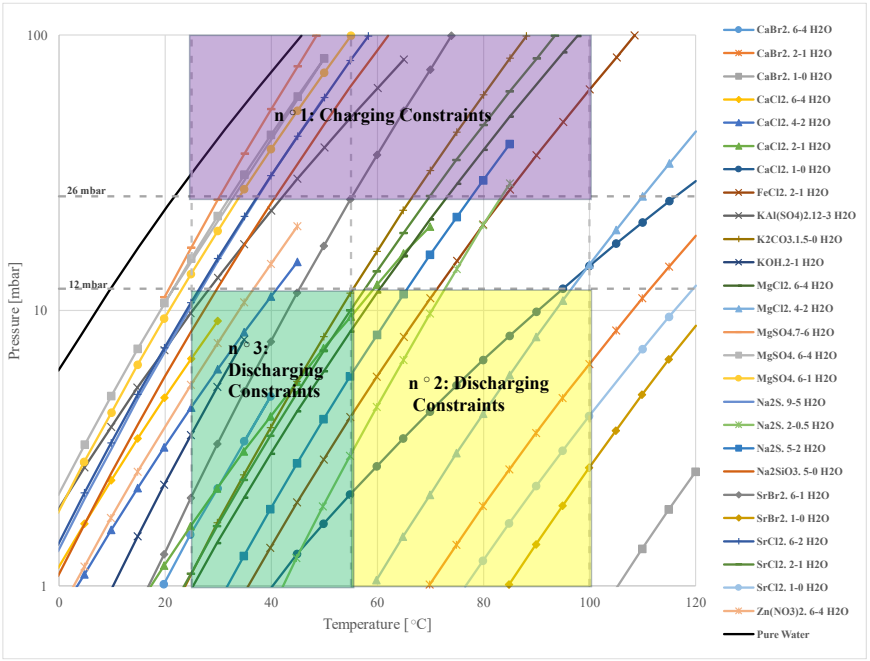

Fig. 5: Equilibrium curves for various solid-gas reactions involving salt hydrates and thermodynamic constraints. To satisfy both charging and discharging constraints (no. 1 and no. 2), the equilibrium curve of the salt must intersect both the charging and discharging constraint areas. Reference data for the equilibrium curves are provided by N'Tsoukpoe *et al.* (2014).

To design the cascade storage unit, it is assumed that the primary salt which can provide the required 55 °C has already been selected ($MgCl_2.6H_2O$), so the focus now shifts to identifying potential materials that could enhance the energy storage density of the process, as targeted by the cascading approach. To qualify:

- The secondary salt must offer a reaction with a higher energy storage density than that of the primary salt ($MgCl_2.6\text{-}4H_2O$, 8.5×10^5 kJ m^{-3}).
- Additionally, the material must meet the discharging constraint no. 3 (Fig. 5): under an evaporator vapor pressure of 1200 Pa (12 mbar), the salt's equilibrium temperature should exceed 25 °C, the minimum outlet temperature of the hot water tank.

Possible salt hydrates that meet these criteria and could be used as secondary salts are listed in Tab. 2. To enhance the energy storage density of the sorption heat storage system, $SrBr_2\cdot6\text{-}1H_2O$ emerges as the most suitable material due to its significantly higher energy storage density. So, strontium bromide is selected as the secondary salt.

Tab. 2: Possible salt hydrates to be used as secondary salt.

Hydrated Salt	$SrBr_2\cdot6H_2O$	$SrCl_2\cdot6H_2O$	$KAl(SO4)_2\cdot12H_2O$	$Na_2SiO_3\cdot5H_2O$
Dehydrated Salt	$SrBr_2\cdot1H_2O$	$SrCl_2\cdot2H_2O$	$KAl(SO4)_2\cdot3H_2O$	$Na_2SiO_3\cdot H_2O$
$T_{melting}$ [°C]	88.6	61.3	65	N.A.
T_{disch} [°C]	45.8	27	28.9	29.8
T_{charge} [°C]	55	37.8	42	43
D_v [kJ m^{-3}]	2.26×10^6	1.58×10^6	1.48×10^6	1.6×10^6

3. Results and discussion

3.1. Single material TCES system

The energy stored and released along with the remaining energy charts of the single material TCES system for Coimbra and Shiraz are shown in Fig. 6 and **Error! Reference source not found.**, respectively. Fig. 6a shows intermittent peaks for energy storage and release events around the middle of the year, particularly noticeable between 4380 hours (mid-year) and 6570 hours (three-quarters of the year) for Coimbra which are much less frequent and have lower magnitudes compared to Shiraz. Fig. 7a exhibits a much higher frequency and

magnitude for energy storage and release for Shiraz compared to Coimbra, indicating a more dynamic energy exchange. The peaks are more frequent and sustained, particularly notable towards the end of the year, which correlates with Shiraz's harsher climate and higher solar radiation levels.

According to Fig. 6b, for Coimbra, the energy released predominantly surpasses the energy stored towards the latter half of the year, leading to low remaining energy values, and the overall trend suggests sporadic energy storage and consistent energy release in the mid to late parts of the year. While for Shiraz, the remaining energy shows a significant rise starting around 3650 hours (roughly mid-year) and peaks around 7300 hours, followed by a gradual decline, Fig. 7b. This indicates substantial energy accumulation in the mid to late parts of the year, consistent with the higher solar energy input due to the climatic conditions of Shiraz. The fact that there is an amount of energy left in the reactor at the end of the year may indicate an oversized reactor design, however, a multiyear simulation would be required to understand how this remaining energy affects the next annual cycle.

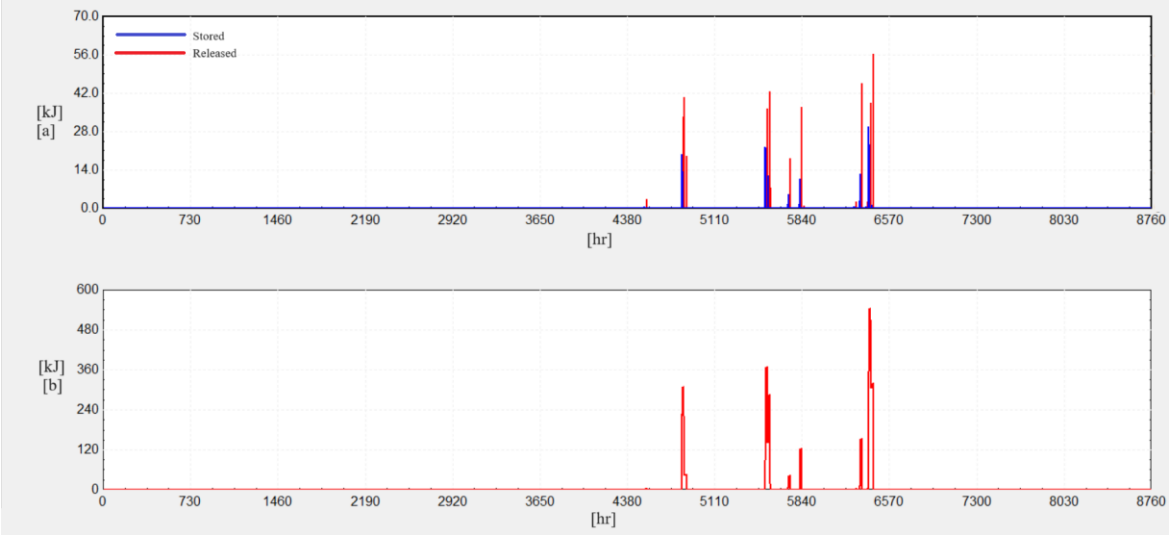

Fig. 6: (a) energy stored and released, and (b) remaining energy of single material TCES system in Coimbra.

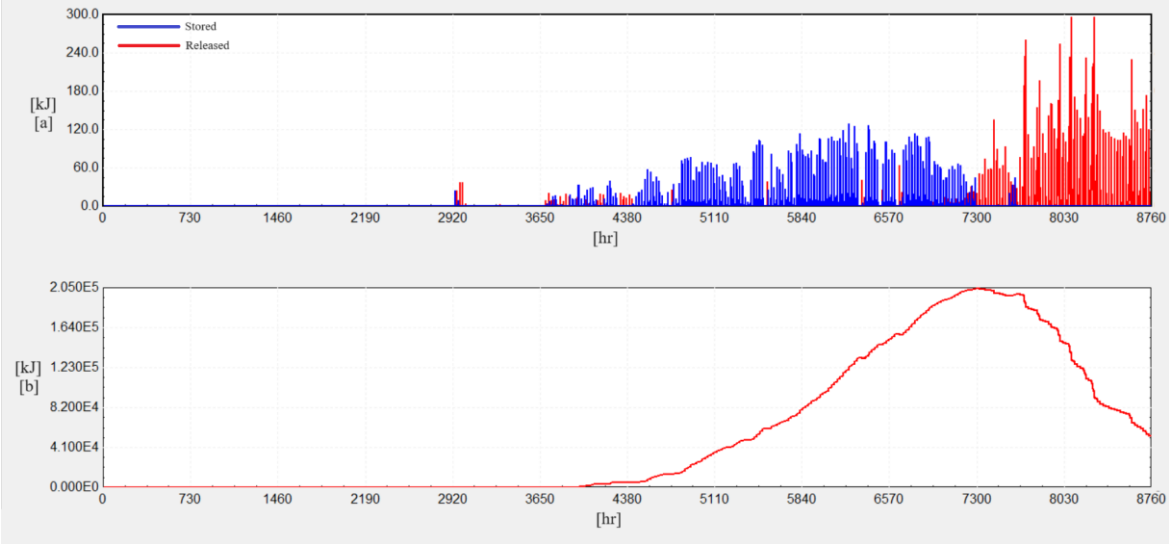

Fig. 7: (a) energy stored and released, and (b) remaining energy of single material TCES system in Shiraz.

The heat transfer rate of the auxiliary heater of the TCES system over a year are depicted for Coimbra and Shiraz in Fig. 8 and Fig. 9, respectively. According to Fig. 8, the auxiliary heater's activity is distributed throughout the year, with notable peaks in the first half. The heat transfer rate fluctuates significantly, reaching up to 3200 kJ h^{-1} frequently. This indicates a substantial need for auxiliary heating due to the inefficiency of

the TCES system. However, under Shiraz weather conditions, the auxiliary heater's activity is concentrated only in the first half of the year (Fig. 9). The heat transfer rate is generally lower compared to Coimbra, with peaks up to 3000 kJ h^{-1}, but less frequently. This suggests less reliance on the auxiliary heater overall, due to higher solar radiation, which also promotes a more effective energy storage in the latter half of the year.

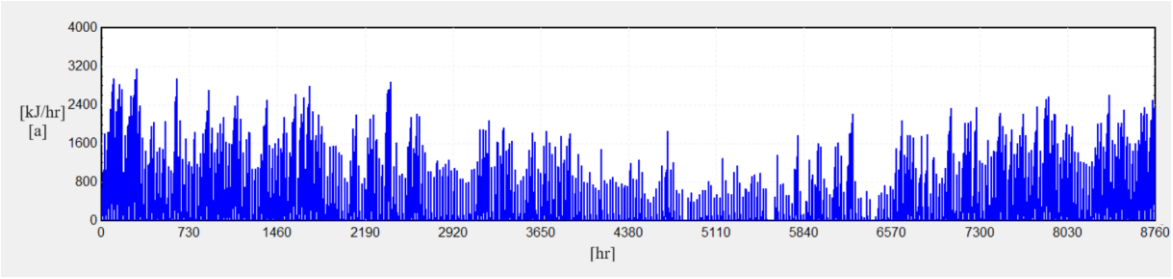

Fig. 8: Heat transfer rate of the auxiliary heater in case of single-material TCES system in Coimbra.

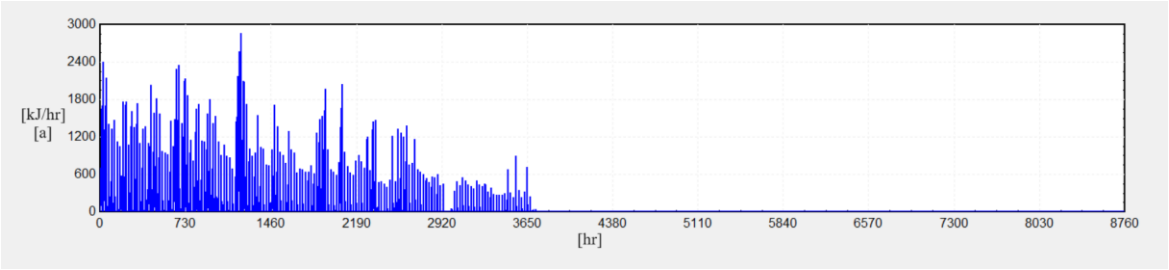

Fig. 9: Heat transfer rate of the auxiliary heater in case of single-material TCES system in Shiraz.

3.2. Cascade TCES system

Fig. 10 depicts the energy storage and release patterns, as well as the remaining energy trend of the cascade sorption energy storage using two thermochemical materials (TCMs): Strontium bromide ($SrBr_2$) and magnesium chloride ($MgCl_2$), for Coimbra during one year. Energy storage patterns are shown in Fig. 10a. For $SrBr_2$ (magenta), energy storage occurs frequently throughout the year with significant peaks, especially between 2000 and 6000 hours. The storage activity reaches up to 180 kJ, indicating substantial energy storage events during these periods. The activity diminishes after 7000 hours, suggesting a seasonal dependency in the latter part of the year. For $MgCl_2$ (yellow), energy storage events are rare and minimal compared to strontium bromide. The peaks are much lower, barely reaching above 60 kJ. This indicates that magnesium chloride is less effective or less utilized for energy storage in this climate.

Energy release patterns are shown in Fig. 10b. For strontium bromide (blue), the energy release is sporadic but notable throughout the year, with peaks up to 240 kJ. There is a consistent pattern of release, particularly between 2000-4500 hours and 6500-8760 hours, indicating a seasonal dependency in the middle part of the year. Also, this aligns with the periods of significant energy storage, indicating active use of stored energy. For magnesium chloride (red), similar to storage, energy release events for are minimal. The release peaks are infrequent and low, barely reaching 60 kJ. This further confirms that $MgCl_2$ plays a minor role in the energy management of the system.

The total remaining energy for strontium bromide shows a steady increase, peaking around 6500 hours at approximately 500,000 kJ (Fig. 10c). After peaking, there is a gradual decline towards the end of the year. This trend suggests efficient storage and gradual utilization of energy throughout the year. The remaining energy for magnesium chloride is negligible, consistent with the low storage and release activity observed. This confirms its minimal contribution to the overall energy storage system.

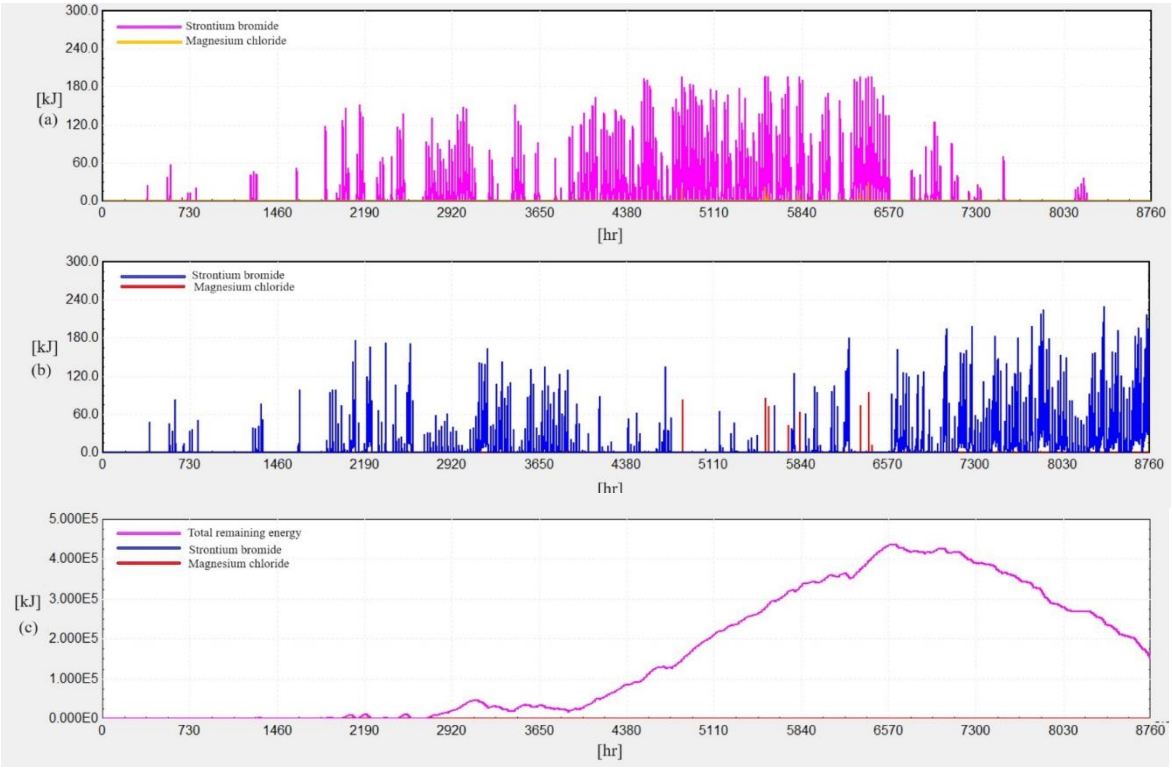

Fig. 10: (a) Energy storage, (b) release patterns, and (c) remaining energy trend of the cascade TCES using two TCMs: Strontium Bromide and Magnesium Chloride, for Coimbra during a year.

Regarding the effectiveness of TCMs, strontium bromide is highly effective in both storing and releasing energy, with substantial activity observed throughout the year. It shows a robust capacity to store energy and release it as needed, maintaining a high level of remaining energy. Magnesium chloride, on the other hand, is ineffective in this setup, with minimal storage and release activity. It has a negligible contribution to the total remaining energy, suggesting it is not suitable for the primary energy storage role in this system mainly due to its high charging temperature which limits its ability to store energy. Thus, the system heavily relies on $SrBr_2$ for energy storage and release, with active periods concentrated between 2000 and 7000 hours. This period represents seasons with significant temperature fluctuations requiring active energy management. The total remaining energy trend indicates efficient energy utilization, with a peak followed by a steady decline, ensuring energy availability throughout the year.

Fig. 11 depicts the energy storage and release patterns, as well as the remaining energy trend of the cascade sorption energy storage using two TCMs, for Shiraz during one year. Regarding the energy storage patterns, shown in Fig. 11a, for strontium bromide (magenta), energy storage occurs frequently throughout the year, with significant peaks, particularly in the second half of the year. The storage activity reaches up to 200 kJ, indicating substantial energy storage events during these periods. Activity diminishes somewhat after 7300 hours, suggesting a seasonal influence on energy storage needs. For magnesium chloride (orange), energy storage events are more frequent and higher compared to Coimbra, though still less than $SrBr_2$. Peaks in storage reach above 120 kJ, indicating a more active role for magnesium chloride in Shiraz compared to Coimbra. This suggests that $MgCl_2$ is more effective or more utilized for energy storage in this system in Shiraz.

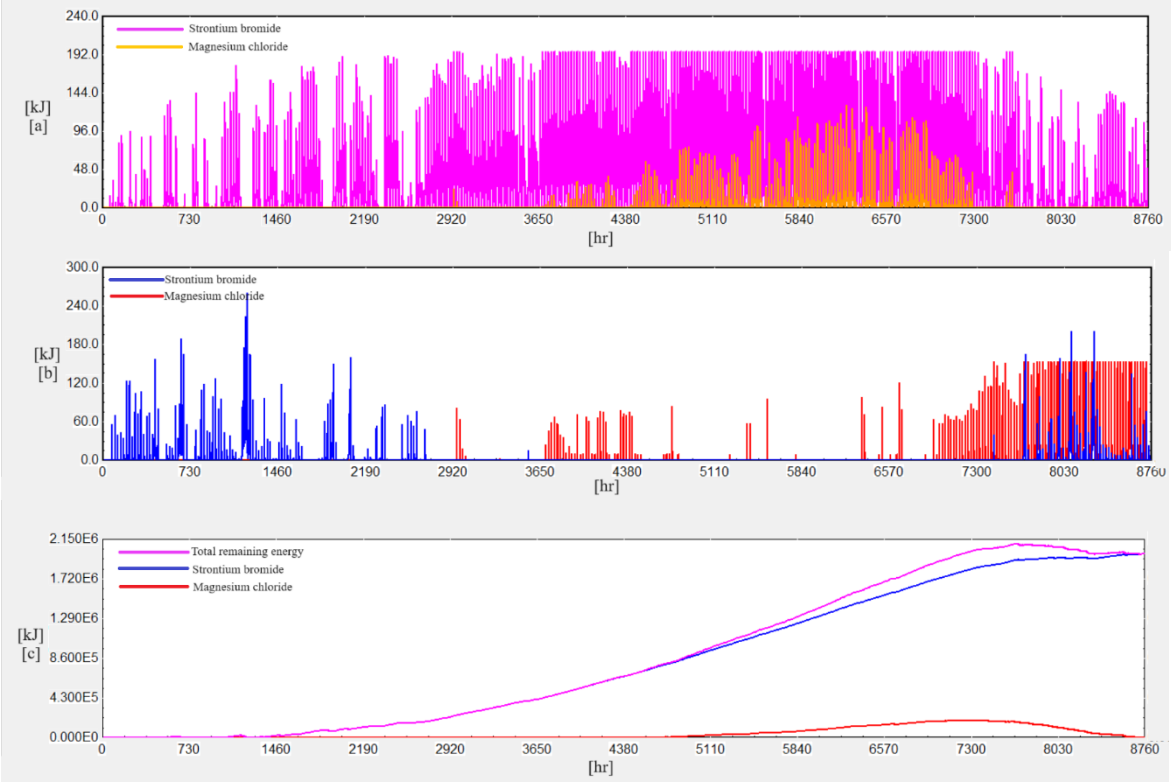

Fig. 11: (a) Energy storage, (b) release patterns, and (c) remaining energy trend of the cascade TCES using two TCMs: Strontium Bromide and Magnesium Chloride, for Shiraz during a year.

Energy release patterns are shown in Fig. 11b. For strontium bromide (blue), the energy release is consistent throughout the year with significant peaks, particularly in the first half of the year. Peaks reach up to more than 240 kJ, indicating active use of stored energy. For magnesium chloride (red), energy release events for are frequent and significant in the second half of the year. The release peaks often reach up to 180 kJ, indicating active involvement in energy management. This further suggests a significant role for $MgCl_2$ in the energy release process in Shiraz.

The total remaining energy for strontium bromide (Fig. 11c) shows a steady increase, peaking around 6500 hours at approximately 2,150,000 kJ. After peaking, there is a gradual decline towards the end of the year. This trend indicates efficient storage and gradual utilization of energy throughout the year. The remaining energy for magnesium chloride increases steadily but remains significantly lower than $SrBr_2$. Peaks at around 7000 hours and then shows a slight decline towards the end of the year. This confirms its supportive role in the overall energy storage system, though less dominant compared to strontium bromide.

Strontium bromide is thus highly effective in both storing and releasing energy, with substantial activity observed throughout the year. It shows a robust capacity to store energy and release it as needed, maintaining a high level of remaining energy. Magnesium chloride is more effective and utilized in Shiraz compared to Coimbra. It plays a significant role in both energy storage and release, especially in the second half of the year. Overall, the system in Shiraz utilizes both TCMs more effectively than in Coimbra, with active periods for both. The total remaining energy trend indicates efficient energy utilization, with peaks followed by a steady decline, ensuring energy availability throughout the year.

The heat transfer rate of the auxiliary heater in case of the cascade TCES system applied in Coimbra and Shiraz are shown in Fig. 12 and Fig. 13, respectively. The auxiliary heater's activity in Coimbra is high in the first half of the year, with peaks reaching up to 3200 kJ h^{-1}. There is a significant amount of auxiliary heating required between 0 and 3650 hours, indicating the need for additional heat to maintain the fluid temperature due to the low amount of stored energy in TCES system to do so. However, after 3650 hours, due to the hours the increasing amount of stored energy beside the seasonal influence, the activity of the auxiliary heater diminishes but still shows sporadic peaks until the end of the year.

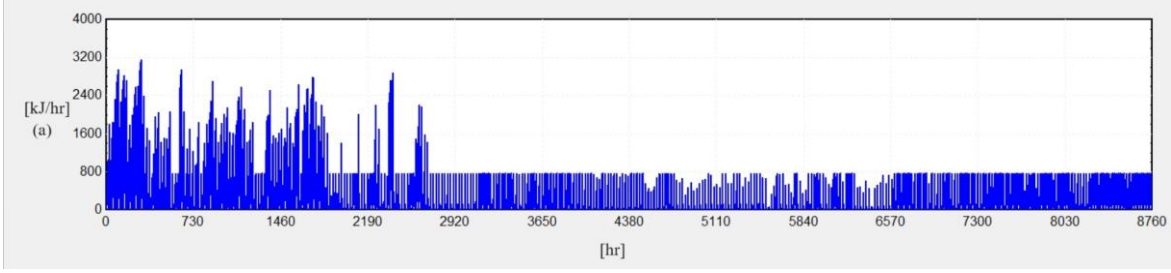

Fig. 12: Heat transfer rate of the cascade TCES system's auxiliary heater in Coimbra.

The auxiliary heater's activity in Shiraz is primarily concentrated in the first 2200 hours of the year, with peaks reaching up to 2400 kJ h^{-1}. After this initial period, the auxiliary heater's activity drops significantly, showing minimal peaks for the remainder of the year until a minor peak at the end. This suggests that Shiraz requires intense auxiliary heating only during a specific period of the year, likely due to distinct seasonal variations and the effectiveness of the thermal storage unit during the latter half of the year, after the TCES system is effectively charged.

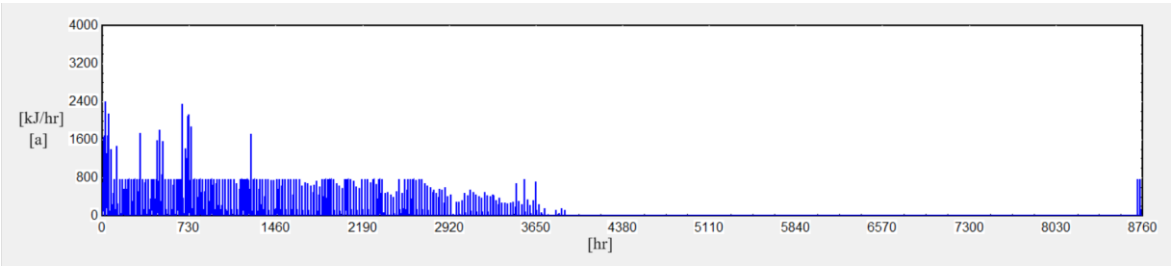

Fig. 13: Heat transfer rate of the cascade TCES system's auxiliary heater in Shiraz.

The performance of the single material and cascade thermochemical energy storage systems is evaluated in the two locations. The results are summarized in Tab. 3. They demonstrate the advantages of the cascade system in terms of auxiliary energy reduction in relation to the conventional system and energy storage capability.

Tab. 3: Performance of the single material and cascade thermochemical energy storage system.

System	Conventional		Single		Cascade	
Location	**Coimbra**	**Shiraz**	**Coimbra**	**Shiraz**	**Coimbra**	**Shiraz**
Ql (Energy rate to load from hot water tank) (kJ)	7.41E+06	9.18E+06	7.41E+06	9.18E+06	7.41E+06	9.18E+06
Qaux (Auxiliary heat supplied by heater) (kJ)	2.71E+06	7.25E+05	2.71E+06	5.27E+05	2.13E+06	4.13E+05
Qs (total stored heat in thermal storage unit) (kJ)	_	_	1.71E+03	2.11E+05	7.12E+05	2.73E+06
Qr (Total released heat from thermal storage unit) (kJ)	_	_	1.71E+03	1.58E+05	5.13E+05	3.84E+05
QS_$MgCl_2$ (Total stored heat in the reacor containing $MgCl_2$ hydrated salt) (kJ)	–	–	–	–	1.71E+03	2.27E+05
QS_$SrBr_2$ (Total stored heat in the reactor containing $SrBr_2$ hydrated salt) (kJ)	–	–	–	–	7.10E+05	2.51E+06

QR_$MgCl_2$ (Total released heat from the reacor containing $MgCl_2$ hydrated salt) (kJ)	–	–	–	–	1.71E+03	2.29E+05
QR_$SrBr_2$ (Total released heat from the reacor containing $SrBr_2$ hydrated salt) (kJ)	–	–	–	–	5.11E+05	1.55E+05
Auxiliary heat reduction percentage in relation to conventional system (%)	–	–	0.1	27.3	21.4	43.1

The cascade system in Coimbra achieved a 21.4% reduction in auxiliary energy demand in relation to the conventional system, compared to only 0.1% for the single material system. Similarly, in Shiraz, the cascade system showed a significant reduction of 43.1%, while the single material system achieved a 27.3% reduction. These results highlight the superior performance of the cascade system in optimizing energy storage and reducing auxiliary energy requirements.

The cascade system's ability to balance the thermodynamic constraints and user requirements allows it to perform more efficiently under varying climatic conditions. The integration of different storage materials in a cascade configuration enables the system to provide the necessary discharge temperature while maintaining a high energy storage density. This makes the cascade thermochemical energy storage system a more viable solution for solar DHW applications. Moreover, as seen in the case of Shiraz, where the system can consistently present a net positive storage rate in the hotter months, it can effectively improve the overall system’s performance, allowing, for example, the storage energy to be used to satisfy other requirements or to be seasonally stored.

Additionally, the analysis of two different TCMs indicates that selecting the primary material based on the local weather conditions and its charging temperature is more advantageous than selecting it based solely on its nominal storage density. In this study, for instance, the charging temperature of $MgCl_2 \cdot 6H_2O$, the primary salt, is approximately 73.8°C. However, in Coimbra, the outlet temperature of the hot water tank rarely reaches this value, rendering magnesium chloride less effective in this climate. Conversely, in Shiraz, where the climate is harsher and the outlet temperature of the hot water tank frequently exceeds the charging temperature of $MgCl_2 \cdot 6H_2O$, this salt proves to be more effective in the cascade system. Therefore, a more detailed analysis of how the charging temperature of the primary TCM impacts the efficiency of the cascade thermochemical energy storage integrated with DHW systems would be highly beneficial.

4. Conclusion

The study evaluates the performance of single material and cascade thermochemical energy storage systems integrated with solar domestic hot water (DHW) systems in different climatic conditions of Coimbra (Portugal) and Shiraz (Iran). The findings indicate that the cascade system, using a combination of $MgCl_2 \cdot 6H_2O$ and $SrBr_2 \cdot 6H_2O$, significantly reduces auxiliary energy demand by 21% in Coimbra and 43% in Shiraz, compared to conventional systems. This reduction underscores the cascade system's efficiency in optimizing energy storage and discharge temperatures. The single material system, while effective, demonstrated limited performance improvements, particularly in milder climates like Coimbra. The cascade configuration's ability to leverage the unique properties of different storage materials enables it to meet the energy demands more effectively, thus enhancing the renewable energy share and overall efficiency of the DHW systems. Additionally, the study highlights the importance of selecting primary thermochemical materials based on local climatic conditions as well as its charging temperature to maximize the system's efficiency, as evidenced by the varying effectiveness of $MgCl_2 \cdot 6H_2O$ in different environments. This comprehensive analysis confirms the viability of cascade thermochemical energy storage systems in improving solar DHW applications, promoting sustainable and efficient energy use. Future work should focus on multi-year simulations and the exploration of other material combinations to further optimize these systems.

5. Acknowledgments

The presented work is framed under the research projects 'AdsorSeason – Long-term adsorption solar thermal energy storage', funded by the Portuguese Foundation for Science and Technology (FCT) (ref. 2022.03339.PTDC, https://doi.org/10.54499/2022.03339.PTDC), and 'Associate Laboratory of Energy, Transports and Aerospace' (ref. UIDB/50022/2020, https://doi.org/10.54499/UIDB/50022/2020). FCT funds Marco S. Fernandes through researcher contract 2021.02975.CEECIND/CP1681/CT0002 (https://doi.org/10.54499/2021.02975.CEECIND/CP1681/CT0002).

6. References

Fernandes, M.S., Brites, G.J.V.N., Costa, J.J., Gaspar, A.R., Costa, V.A.F., 2016. Modeling and parametric analysis of an adsorber unit for thermal energy storage. Journal of Energy. 102, 83-94. https://doi.org/10.1016/j.energy.2016.02.014.

Fuentes, E., Arce, L., Salom, J., 2018. A review of domestic hot water consumption profiles for application in systems and buildings energy performance analysis. Journal of Renewable and Sustainable Energy Reviews. 81, Part 1, 1530-1547. https://doi.org/10.1016/j.rser.2017.05.229.

N'Tsoukpoe, K.E., Mazet, N., Neveu, P., 2016. The concept of cascade thermochemical storage based on multimaterial system for household applications. Journal of Energy and Buildings. 129, 138-149. https://doi.org/10.1016/j.enbuild.2016.07.047.

N'Tsoukpoe, K.E., Schmidt, T., Rammelberg, H. U., Watts, B. A., Ruck, W.K.L., 2014. A systematic multi-step screening of numerous salt hydrates for low temperature thermochemical energy storage, Journal of Applied Energy, 124, 1-16, https://doi.org/10.1016/j.apenergy.2014.02.053.

Scapino, L., Zondag, H. A., Van Bael, J., Diriken, J., Rindt, C.C.M., 2017. Sorption heat storage for long-term low-temperature applications: A review on the advancements at material and prototype scale. Journal of Applied Energy. 190, 920-948. https://doi.org/10.1016/j.apenergy.2016.12.148.

Stitou, D., Goetz, V., Spinner, B., 1997. A new analytical model for solid-gas thermochemical reactors based on thermophysical properties of the reactive medium, Chemical Engineering and Processing: Process Intensification, 36, Issue 1,29-43, ISSN 0255-2701, https://doi.org/10.1016/S0255-2701(96)04173-6.

Xu, J., Li, T., Yan, T., Chao, J., Wang, R., 2021. Dehydration kinetics and thermodynamics of magnesium chloride hexahydrate for thermal energy storage. Solar Energy Materials and Solar Cells.219, 110819, ISSN 0927-0248, https://doi.org/10.1016/j.solmat.2020.110819.

Yan, T., Zhang, H., 2022. A critical review of salt hydrates as thermochemical sorption heat storage materials: Thermophysical properties and reaction kinetics. Journal of Solar Energy. 242, 157-183, ISSN 0038-092X, https://doi.org/10.1016/j.solener.2022.07.002.